A&A 392, 575–584 (2002)
DOI: 10.1051/0004-6361:20020938

Astronomy & Astrophysics

Stellar evolution with rotation

IX. The effects of the production of asymmetric nebulae on the internal evolution

A. Maeder⋆

Geneva Observatory, 1290 Sauverny, Switzerland

Received 8 April 2002 / Accepted 19 June 2002

Abstract. The anisotropies of the mass loss by stellar winds, which lead to asymmetric nebulae, influence the loss of angular momentum. Polar enhanced mass loss is embarking less angular momentum than isotropic mass loss, while equatorial mass loss is removing more angular momentum. Thus, the evolution of a star and of its rotation is also influenced by the anisotropies. We give the basic equations expressing the evolution of the angular momentum for a rotating star experiencing mass loss by anisotropic stellar winds, with account for differential rotation, meridional circulation and shear diffusion. In the general case, the outer layers must be studied with a time dependent boundary conditions. However, for low enough mass loss rates, a stationary situation can be established at the stellar surface. It implies a positive Ω–gradient for polar mass loss and a negative Ω–gradient for a dominant equatorial mass loss. At the opposite, for extremely high mass loss rates (like for LBV and WR stars), the outer layers are removed before the torque associated to the anisotropies has the time to be transmitted inward.
We show that for the fastest rotating O-type stars (between 25 and 60 $M_\odot$ and for an average rotation velocity during the MS phase $\upsilon \geq 300$ km s^{-1}), the anisotropies of the mass loss may significantly influence the evolution of the stellar velocities and may lead the stars to break–up.

Key words. stars: rotation – stars: evolution –stars: mass–loss

1. Introduction

Generally in stellar evolution, it is considered that "details" concerning the stellar surface, like the anisotropies of the stellar flux, do not affect the internal stellar evolution. The well known reason, as evidenced in basic textbooks, is that the outer boundary conditions have less and less influence as we consider deeper stellar layers. We shall show here that the anisotropies of the radiation flux at the stellar surface may in some cases significantly affect the evolution of a massive star.

The anisotropies of the radiation flux in a rotating star result from the von Zeipel theorem (von Zeipel 1924; for the case of differential rotation, see also Maeder 1999). This theorem essentially says that the local flux on a rotating star is proportional to the effective local gravity $g_{\rm eff}$. Thus, the flux is higher at the pole and weaker at the equator, and so does also the effective temperature $T_{\rm eff}$.

Such differences of $T_{\rm eff}$ over the stellar surface also influence the local flux of mass loss (see also Pelupessy et al. 2000). Models of radiation driven winds from rotating stars with account of 2–D and non–LTE effects have also been recently developed by Petrenz & Puls (2000). The analytical expressions of the theory of stellar winds on a rotating star have been developed by Maeder & Meynet (2000). The main result is that the mass flux shows large deviations from spherical symmetry, with 2 main factors causing the anisotropies: 1) The higher polar $T_{\rm eff}$ favours polar mass ejections ($g_{\rm eff}$–effect). 2) The lower equatorial $T_{\rm eff}$ may lead to larger opacities, thus favouring higher equatorial mass loss or even leading to an equatorial ring ejection (κ–effect). The relative importance of these two effects depends on rotation and on the average stellar $T_{\rm eff}$. In O–type and early B–type stars, the opacity is mainly electron scattering opacity and thus there is little or no significant equatorial enhancement of the opacity, and thus in general the main effect is the $g_{\rm eff}$–effect, which leads to bipolar outflows. An equatorial ejection with the formation of an equatorial ring is likely to occur when the equatorial regions become cooler than $T_{\rm eff}$ = 21 500 K (corresponding to spectral type B1.5). Then there are rapid opacity growths or jumps (called bi–stability limits) where the force multipliers (see Lamers et al. 1995; Kudritzki & Puls 2000) characterising the opacities undergo strong changes.

Most nebulae ejected by stars are asymmetric. This is the case for the nebulae around LBV stars, like η Carinae or AG Carinae (cf. Nota & Clampin 1997; cf. also Lamers et al. 2001), which show large bi–polar outflows or "peanut shaped" nebulae. Asymmetries are also generally present in the nebulae

⋆ e-mail: andre.maeder@obs.unige.ch

around WR stars, in the shell ejection by Be stars and in the planetary nebulae, etc. A polar ejection removes only a little amount of angular momentum, while an equatorial ejection removes a lot of angular momentum. Thus, the amount of angular momentum remaining in massive stars after a phase of heavy mass loss depends very much on the anisotropies of the mass loss rates. As rotation influences the output of stellar evolution (cf. Meynet & Maeder 2000), we conclude that the anisotropies of the stellar winds may in some cases also influence the course of stellar evolution.

The object of this work is to give the basic equations for accounting for the anisotropies of the stellar winds, in a way consistent with the equations expressing the transport of angular momentum by meridional circulation and shears. We want also to make some numerical tests to examine the feasibility of the proposed scheme and to explore some first consequences of the anisotropies of the mass loss. Section 2 gives the basic equations for the general case. Section 3 examines some stationary solutions. Section 4 gives the expression of the external torque in the case of anisotropic wind compared to the case of isotropic wind. In Sect. 5 we make some numerical tests and illustrations.

2. The basic equations for the outer stellar layers

The basic equation for the conservation of angular momentum for a stellar layer is (cf. Zahn 1992)

$$\frac{\partial}{\partial t}\left(\rho r^2\overline{\Omega}\right)_r = \frac{1}{5r^2}\frac{\partial}{\partial r}\left(\rho r^4\overline{\Omega}U(r)\right) + \frac{1}{r^2}\frac{\partial}{\partial r}\left(\rho \nu r^4\frac{\partial\overline{\Omega}}{\partial r}\right). \quad (1)$$

The quantity $\overline{\Omega}$ is the average angular velocity over the considered isobar. The so–called approximation of shellular rotation is made, it assumes that $\overline{\Omega}$ is essentially a function of r, because the differential rotation on an isobar is small. The physical reason for this assumption rests on the strong horizontal turbulence in a differentially rotating star. Indeed, I am not fully convinced that the currently used coefficient of horizontal turbulence, as proposed by Zahn (1992), is high enough to garantee the homogeneity of the angular velocity on an equipotential. Thus, the basic physics and assumptions underlaying the derivations of this coefficient are being re–examined (Maeder 2002). This appears to result in a new expression for the coefficient of horizontal turbulence, which happens to be at least one order of a magnitude higher. As a consequence, the assumption of shellular rotation as originally proposed by Zahn (1992) will be reinforced.

The above equation expresses that the change of angular momentum of a certain mass element in a star results from the transport by the meridional circulation with a velocity $U(r)$ and from the turbulent diffusion with a coefficient ν. If $U(r)$ and ν are zero, this equation just says that the specific angular momentum $r^2\overline{\Omega}$ of a mass element remains constant. The expression for $U(r)$ is that given by Maeder & Zahn (1998) and for ν by Maeder & Meynet (2001).

If the anisotropic stellar winds remove some matter, for example, at the pole, the lack of mass, say the "hole" at the pole, will be filled almost instantaneously by some material moving horizontally on the equipotential and bringing its angular momentum. Indeed, the timescale for this compensation is very short. It is the local dynamical timescale, of the orders of hours or days at most in massive stars. Thus, the equation of the surface will always be an equipotential, given for example by the Roche model. However, in the above example the polar mass loss removes less angular momentum than the corresponding amount of mass lost spherically. Let us call $\dot{\mathcal{L}}_{\rm excess}$ the difference of the angular momentum lost by unit of time between an anisotropic stellar wind and a spherical wind for the same amount of mass loss in a star of given angular velocity $\overline{\Omega}$

$$\dot{\mathcal{L}}_{\rm excess}(\overline{\Omega}) = \dot{\mathcal{L}}_{\rm anis}(\overline{\Omega}) - \dot{\mathcal{L}}_{\rm iso}(\overline{\Omega}), \quad (2)$$

where $\dot{\mathcal{L}}_{\rm anis}(\overline{\Omega})$ and $\dot{\mathcal{L}}_{\rm iso}(\overline{\Omega})$ are the rates of losses of the angular momentum by the anisotropic and isotropic winds respectively; these are negative values.

Whether anisotropic mass loss is present or not, the basic Eq. (1) for the conservation of angular momentum remains the same in the stellar interior. The external torque $\dot{\mathcal{L}}_{\rm excess}(\overline{\Omega})$ due to an anistropic mass loss is only *directly* acting on the outer surface layer. This means that the modifications of the system of equations only concern the outer boundary conditions. Of course indirectly, the change of boundary conditions can affect the internal distribution of $\overline{\Omega}(r)$, the patterns of meridional circulation, the evolution, etc.

Focusing on the outer boundary conditions, we integrate Eq. (1) over the last thin shell of mass $M_{\rm shell}$ centered at a level r just below the stellar surface. We get with account for the anisotropic loss of angular momentum by stellar winds at the surface,

$$\frac{\mathrm{d}}{\mathrm{d}t}\left(M_{\rm shell}\overline{\Omega}\, r^2\right) = -\frac{4\pi}{5}\,\rho r^4\overline{\Omega}U(r) - 4\pi\,\rho\nu r^4\frac{\partial\overline{\Omega}}{\partial r} + \frac{3}{2}\dot{\mathcal{L}}_{\rm anis}. \quad (3)$$

We can derive the left hand side term

$$\frac{\mathrm{d}}{\mathrm{d}t}\left(M_{\rm shell}\overline{\Omega}\, r^2\right) = \dot{M}_{\rm shell}\overline{\Omega}\, r^2 + M_{\rm shell}\frac{\mathrm{d}}{\mathrm{d}t}\left(\overline{\Omega}\, r^2\right), \quad (4)$$

where the first term on the right corresponds to the rate of the loss of angular momentum taken by the isotropic mass loss. If we assume that the mass ejected spherically is just embarking its own angular momentum, one has the equality

$$\frac{2}{3}\dot{M}_{\rm shell}\,\overline{\Omega}\, r^2 = \dot{\mathcal{L}}_{\rm iso}. \quad (5)$$

Now, if we substract this isotropic component on both sides of Eq. (3), we get

$$M_{\rm shell}\frac{\mathrm{d}}{\mathrm{d}t}\left(\overline{\Omega}\, r^2\right) = -\frac{4\pi}{5}\rho r^4\overline{\Omega}U(r) - 4\pi\,\rho\nu r^4\frac{\partial\overline{\Omega}}{\partial r} + \frac{3}{2}\dot{\mathcal{L}}_{\rm excess}. \quad (6)$$

If $U(r) > 0$, the circulation removes angular momentum from the outer shell to bring it toward the interior; if $\frac{\partial\overline{\Omega}}{\partial r} > 0$, the diffusion does the same. In addition, there is a contribution $\frac{3}{2}\dot{\mathcal{L}}_{\rm excess}$, which may be positive or negative, because the anisotropic mass loss may take away less or more angular momentum than the spherically symmetric case.

For polar mass loss, the contribution to the rotation of the outer shell is positive, i.e.

$$\frac{3}{2}\dot{\mathcal{L}}_{\rm excess} > 0, \quad (7)$$

because $|\dot{\mathcal{L}}_{\rm anis}(\overline{\Omega})| < |\dot{\mathcal{L}}_{\rm iso}(\overline{\Omega})|$ in this case. This means the following: the removal of some mass by polar stellar winds embarks less angular momentum that for an equivalent spherical mass loss. Thus, this is as if we add some angular momentum on the last remaining layer. Conversely, for equatorial mass loss we have

$$\frac{3}{2}\dot{\mathcal{L}}_{\rm excess} < 0. \tag{8}$$

In this case, the equatorial mass loss pumps more angular momentum than the equivalent spherical mass loss and this accelerates the braking of stellar rotation. In Sect. 4 below, we give the appropriate expression for $\dot{\mathcal{L}}_{\rm excess}$ in the general case of anisotropic mass loss.

We insist on the fact that Eq. (6) is not just a mathematical trick to account for the anisotropic mass loss, but it closely corresponds to the physical conditions in the case of anisotropic mass loss. Let us, for example, consider the case of polar enhanced mass loss. As said above, the mass removed by stellar winds at the pole will be almost instantaneously replaced by a flow of material coming from equatorial regions on the equipotential. This material will have more angular momentum than the average material on the equipotential and thus it exerts a positive torque on the surface layer, enhancing its rotation. The strong horizontal turbulence rapidly smears out the effect of this torque on the considered equipotential. We do think that this one dimensional treatment of a physical problem, which by essence is two dimensional, is a correct although simplified representation. The two hypotheses, a) of the instantaneous replacement of the matter on a surface layer and b) that this layer is preserving its equipotential shape, do not seem unreasonable in view of the considered dynamical timescales. Of course, very critical would be the presence of magnetic field which would introduce some coupling of the surface layer both upwards with the ejected matter and downwards with the layers below, as well as horizontally on the equipotential. In this context, let us note that Eq. (6) can also be applied in stars, which are slowed down by magnetic braking. In this case the quantity $\dot{\mathcal{L}}_{\rm excess}$ is the torque exerted by the magnetic field.

There is an additional problem in massive stars. If the mass loss is high, the outer layers are removed before the transport of angular momentum by circulation and turbulent diffusion has the time to bring the angular momentum inward. The condition for the transport of angular momentum to occur is that the characteristic time t_Ω for the readjustement of $\overline{\Omega}(r)$ by circulation and diffusion is shorter than the caracteristic timescale $t_{\dot{M}}$ for mass loss, i.e.

$$t_\Omega < t_{\dot{M}}. \tag{9}$$

For an outer shell of mass thickness ΔM, one has $t_{\dot{M}} \simeq \frac{\Delta M}{(-\dot{M})}$. Usually in stellar interiors, the meridional circulation is more efficient that turbulent mixing to transport the angular momentum. However, as shown below in Sect. 3.2, the thermal timescale at the surface of massive stars becomes so small that the departure from thermal equilibrium in rotating stars will not contribute to the driving of circulation, thus $U(r) = 0$ is a good approximation at the stellar surface. Thus, one may write for the characteristic time $t_\Omega = \frac{(\Delta r)^2}{\nu \frac{|\Delta\Omega|}{\Omega}}$. Thus, the condition (9) means that the actual mass loss rate $\dot{M}$ must be smaller in absolute values than a critical mass loss $\dot{M}_{\rm crit}$,

$$\dot{M}_{\rm crit} = -\left|\frac{\nu}{\Omega}\frac{\Delta M}{\Delta r}\frac{\Delta\Omega}{\Delta r}\right| = -4\pi\,\overline{\rho}\,r^2\nu\left|\frac{\frac{\Delta\Omega}{\Omega}}{\Delta r}\right|. \tag{10}$$

Thus, if this condition is not realised the external torque $\dot{\mathcal{L}}_{\rm excess}$ will have no effect, since the layers will have been lost before they are able to transfer toward the interior the excess or lack of angular momentum which is applied at their surface. From the numerical example discussed in Sect. 4, we may estimate that the order of magnitude of $\dot{M}_{\rm crit}$ is of the order of $-10^{-5}\ M_\odot\ {\rm yr}^{-1}$ which corresponds to an initial mass of about 100 $M_\odot$. This means that in the most massive stars, as well as in LBV and WR stars, the mass loss rates are so high that there is little or no transfer of the excess (or lack) of angular momentum into the underlaying layers. Thus, the effects due to the anisotropic mass loss are likely not important for the internal evolution of these extreme stars, provided they have no magnetic field. However, the anisotropies of mass loss will of course shape the ejected nebulae.

3. Stationary solutions

3.1. Zahn's solution

This solution applies to the outer boundary of the radiative zone in solar type stars, which have an external convective zone. An asymptotic regime, where the wind properties vary only slowly, on a time long with respect to the characteristic time of meridional circulation is considered by Zahn (1992). He also assumes, which is well verified, that the momentum of inertia of the boundary layer is negligible, so that the flux of angular momentum is nearly constant with depth. Thus, the time derivative in Eq. (6) is zero. In addition, Zahn assumes that the angular momentum transported by the turbulent viscosity is negligible with respect to the advection, an assumption which is also verified in the interior. Thus, one has

$$\frac{\partial\Omega}{\partial r} = 0. \tag{11}$$

From Eq. (6) one is left with

$$U(r) = \frac{15}{8\pi}\frac{\dot{\mathcal{L}}_{\rm excess}}{\rho r^4\overline{\Omega}}. \tag{12}$$

The two Eqs. (11) and (12) form, according to Zahn, the outer boundary conditions of the internal radiative zone in models of solar type stars. We note that if $\dot{\mathcal{L}}_{\rm excess} = 0$, then $U(r) = 0$ and with $\frac{\partial\Omega}{\partial r} = 0$, one has again the two boundary conditions usually employed in stellar models, (cf. Talon et al. 1997; Meynet & Maeder 2000).

If $\dot{\mathcal{L}}_{\rm excess} < 0$, as it would be produced for example by the magnetic braking in solar type stars, then one has $U(r) < 0$ near the outer edge of the radiative zone. This means that the lack of angular momentum at the edge will be compensated by a meridional circulation flow descending along the polar axis and ascending at the equator. It may be surprising to have a non zero $U(r)$ at the outer boundary. But as pointed by Zahn (1992), there is no problem since in solar type stars the outer convective zone allows the return of mass and its conservation.

3.2. Boundary conditions for upper Main Sequence stars

Future works will tell us whether the above boundary conditions are well appropriate for solar type stars. In the case of Main Sequence (MS) stars with outer radiative layers, the above boundary conditions do not apply for two reasons. Firstly, with a non zero value of $U(r)$ the return of mass is not insured; one cannot consider that the mass loss insures the mass continuity, because stellar winds in massive stars are present independently of the sign of $U(r)$. Secondly, we may not consider that $\frac{\partial\Omega}{\partial r} = 0$, since the positive or negative torque exerted by $\dot{\mathcal{L}}_{\rm excess}$ in the case of anisotropic stellar winds will create a gradient of Ω in the outer layers. Thus, more appropriate boundary conditions have to be found.

The content of angular momentum of the outer shell is relatively very small, or in other words there is no possibility of stockage in the outer shell. Thus a situation of equilibrium may be reached between the gain (or loss) $\dot{\mathcal{L}}_{\rm excess}$ of angular momentum due to the anisotropic loss and the transport due to advection or diffusion toward (or from) the deeper layers. Thus, we consider that in the external shell the time derivative in the first member of Eq. (6) is zero and we have

$$\frac{3}{8\pi}\dot{\mathcal{L}}_{\rm excess} = +\frac{1}{5}\,\rho r^4\overline{\Omega}U(r) + \rho\nu r^4\frac{\partial\overline{\Omega}}{\partial r}\cdot \quad (13)$$

In the deep interior, it is well known that meridional circulation is the most efficient process for transporting the angular momentum. However, this is not necessarily the case very close to the stellar surface. Indeed, meridional circulation results from a departure from thermal equilibrium on an isobar, which drives some motions. However, close to the stellar surface, the timescale for thermal adjustment is

$$t_{\rm therm} \sim \frac{(\Delta r)^2}{K} \sim \frac{3\kappa\rho^2 c_{\rm P}(\Delta r)^2}{4acT^3}, \quad (14)$$

where K is the thermal diffusivity. The timescale $t_{\rm therm}$ may become smaller than the local dynamical time $t_{\rm dyn} \sim \frac{1}{\sqrt{G\rho}}$. Let us examine the ratio of these two timescales

$$\frac{t_{\rm therm}}{t_{\rm dyn}} \sim \left(\frac{3\kappa c_{\rm P}G^{\frac{1}{2}}}{4ac}\right)\frac{\rho^{\frac{5}{2}}}{T^3}(\Delta r)^2. \quad (15)$$

To know how the pressure P is varying close to the surface, we divide the equation of hydrostatic equilibrium by the equation of radiative equilibrium. This leads to

$$\frac{{\rm d}P}{{\rm d}T} = \frac{16\pi acGMT^3}{3\kappa L}\cdot \quad (16)$$

For electron scattering opacity, this gives $P \sim T^4$. One also has $\beta P = \frac{k}{\mu m_{\rm H}}\rho T$, where β is the ratio of the gas pressure to the total pressure P. Thus $T^3 \sim \frac{\rho}{\beta}$ and

$$\frac{t_{\rm therm}}{t_{\rm dyn}} \sim \beta\rho^{\frac{3}{2}}. \quad (17)$$

At the stellar surface, ρ and β go to zero, which shows that the thermal time scale becomes shorter than the dynamical timescale. Thus, near the stellar surface a departure of thermal equilibrium will be restored very quickly by radiative transfer, without requiring the driving of circulation currents like the meridional circulation. Therefore, one of the boundary conditions at the surface radius R is just

$$U(R) = 0, \quad (18)$$

and thus from Eq. (13), one has

$$\frac{\partial\Omega}{\partial r} = \frac{3}{8\pi}\frac{\dot{\mathcal{L}}_{\rm excess}}{\rho\nu r^4}\cdot \quad (19)$$

Equations (18) and (19) form the appropriate outer boundary conditions for stationary situations in stars with radiative layers near the surface. One sees that if $\dot{\mathcal{L}}_{\rm excess} > 0$ (polar ejection), one has Ω growing with r at the edge of the star. This is what is expected, since then some rotation is added at the boundary and is thus able to diffuse toward the interior. This is consistent with the fact that at the surface the main transport of angular momentum is by diffusion, since as we have seen $U(R) = 0$. Conversely, for a dominant equatorial mass loss or for magnetic braking, we shall have $\frac{\partial\Omega}{\partial r} < 0$ and the diffusion of angular momentum toward the exterior will be favoured. Consistently, if $\dot{\mathcal{L}}_{\rm excess} = 0$ we have again the usual conditions $U(R) = 0$ and $\frac{\partial\Omega}{\partial r} = 0$.

As shown by Eqs. (9) and (10), the mass loss rates must not be too large in order that the outer layers are not removed before they have had the time to transport the angular momentum. This requirement is even much more severe for an equilibrium stage to be established and we may estimate that mass loss rates smaller by about 2 orders of a magnitude with respect to $\dot{M}_{\rm crit}$ are necessary for this. In view of the estimate given after Eq. (10), this means that the mass loss rates must likely be smaller than $\sim 10^{-7}\ M_\odot\ {\rm yr}^{-1}$, which corresponds to stellar mass lower than about 15 $M_\odot$. These are rough estimates and future grids of models may further precise these values.

4. The difference of angular momentum losses between anisotropic and isotropic winds

We need now to express the quantity $\dot{\mathcal{L}}_{\rm excess}$ appearing in the previous sections. According to the definition, one has

$$\dot{\mathcal{L}}_{\rm excess} = \left[\dot{I}_{\rm anis}(\overline{\Omega}) - \dot{I}_{\rm iso}(\overline{\Omega})\right]\overline{\Omega} = \overline{\Omega}\,\dot{I}_{\rm iso}(\overline{\Omega})\left[\frac{\dot{I}_{\rm anis}(\overline{\Omega})}{\dot{I}_{\rm iso}(\overline{\Omega})} - 1\right], \quad (20)$$

where $\dot{I}_{\rm iso}(\overline{\Omega})$ and $\dot{I}_{\rm anis}(\overline{\Omega})$ are the time variations (negative values) of the momentum of inertia due to the mass loss by isotropic and anisotropic stellar winds respectively. The momentum of inertia $I_{\rm iso}(\overline{\Omega})$ in a shell between the radii r_1 and r_2 in a star rotating with angular velocity $\overline{\Omega}$ is

$$I_{\rm iso}(\overline{\Omega}) = 2\pi\int_0^{\pi}\int_{r_1}^{r_2}\frac{r^4(\overline{\Omega},\vartheta)\rho\sin^3\vartheta}{\cos\epsilon}{\rm d}\vartheta{\rm d}r. \quad (21)$$

For a thin spherical shell of radius R and mass ΔM, $I_{\rm iso}$ is just the usual expression

$$I_{\rm iso} = \frac{2}{3}R^2\Delta M. \quad (22)$$

In a rotating star, the radial direction does not in general coincide with the normal to the surface (direction of the gravity). The angle ϵ between the radial direction and the direction of the effective gravity is a function of Ω and ϑ, it is given by

$$\cos\epsilon = -\frac{\boldsymbol{g}_{\mathbf{eff}} \cdot \boldsymbol{r}}{|\boldsymbol{g}_{\mathbf{eff}} \cdot \boldsymbol{r}|} = \left(\frac{1}{x^2(\omega,\vartheta)} - \frac{8}{27}\omega^2 x(\omega,\vartheta)\sin^2\vartheta\right)\psi^{-\frac{1}{2}} \quad (23)$$

with

$$\psi = \left(-\frac{1}{x^2(\omega,\vartheta)} + \frac{8}{27}\omega^2 x(\omega,\vartheta)\sin^2\vartheta\right)^2 + \left(\frac{8}{27}\omega^2 x(\omega,\vartheta)\sin\vartheta\cos\vartheta\right)^2. \quad (24)$$

The effective gravity $\boldsymbol{g}_{\mathbf{eff}}$ includes the effect of the gravitational potential and centrifugal force, but not the effect of radiation pressure (cf. Maeder & Meynet 2000). The rotation parameter ω is the fraction of the angular break–up velocity. The quantity $x(\omega,\vartheta)$ is the ratio of the radius at colatitude ϑ with respect to the polar radius $R_{\rm pb}$ at break–up velocity. (Remark: the exact value of the polar radius $R_{\rm p}(\omega)$ also slightly depends on rotation through the structural equations; this effect is accounted for in the numerical models.) The value of $x(\omega,\vartheta)$ is a solution of the equation of the stellar surface in the Roche approximation for given values of ω and colatitude ϑ, i.e.

$$\frac{1}{x(\omega,\vartheta)} + \frac{4}{27}\omega^2 x^2(\omega,\vartheta)\sin^2\vartheta = \frac{R_{\rm p}(\omega)}{R_{\rm pb}}. \quad (25)$$

$$\text{with } x(\omega,\vartheta) = \frac{r(\overline{\Omega},\vartheta)}{r_{\rm p}} \quad \text{and} \quad \omega^2 = \frac{\overline{\Omega}^2 r_{\rm eb}^3}{GM}. \quad (26)$$

$r_{\rm eb}$ is the equatorial radius at break–up. The time variation of the momentum of inertia by a star which loses mass at a rate $\dot{M}$ over its actual surface Σ is

$$\dot{I}_{\rm iso}(\overline{\Omega}) = 2\pi \int_\Sigma r^2(\overline{\Omega},\vartheta)\sin^2\vartheta \, {\rm d}\dot{M}. \quad (27)$$

The quantity ${\rm d}\dot{M}$ is defined by the local mass flux. Usually an isotropic mass flux is considered in the stellar wind theory. However, for the reasons expressed in Sect. 1, the mass loss in a rotating star is anisotropic. Depending on whether we consider the isotropic or anisotropic cases, we have

$${\rm d}\dot{M} = \left(\frac{\Delta\dot{M}(\overline{\Omega},\vartheta)}{\Delta\sigma}\right)_{\rm iso/anis} {\rm d}\sigma, \quad (28)$$

where ${\rm d}\sigma$ refers to the surface element on the rotating star. Thus, the corresponding expression for the time variation of the momentum of inertia is in the isotropic or anisotropic case

$$\dot{I}_{\rm iso/anis}(\overline{\Omega}) = 2\pi \int_0^\pi \left(\frac{\Delta\dot{M}(\overline{\Omega},\vartheta)}{\Delta\sigma}\right)_{\rm iso/anis} \frac{r^4(\vartheta)\sin^3\vartheta}{\cos\epsilon}{\rm d}\vartheta. \quad (29)$$

The expression for the anisotropic mass flux has been obtained by the application of the stellar wind theory to a rotating star (cf. Maeder & Meynet 2000), by taking into account the variations of $T_{\rm eff}$ and effective gravity with latitude and the change of the local Eddington factor. Also, the force multipliers k and α (cf. Castor et al. 1975; Lamers et al. 1995; Puls et al. 1996), which characterize the stellar opacity, may vary over the stellar surface since the temperature and gravity are varying,

$$\left(\frac{\Delta\dot{M}(\overline{\Omega},\vartheta)}{\Delta\sigma}\right)_{\rm anis} \simeq A \left[\frac{L(P)}{4\pi GM_\star(P)}\right]^{\frac{1}{\alpha}} \frac{g_{\rm eff}[1+\zeta(\vartheta)]^{\frac{1}{\alpha}}}{(1-\Gamma_\Omega(\vartheta))^{\frac{1}{\alpha}-1}}$$

$$\text{with} \quad A = (k\alpha)^{\frac{1}{\alpha}}\left(\frac{1-\alpha}{\alpha}\right)^{\frac{1-\alpha}{\alpha}}. \quad (30)$$

The Eddington factor $\Gamma_\Omega(\vartheta)$ in a rotating star must be defined in an appropriate way, i.e. as the ratio of the *local* flux to the limiting *local* flux. In this way, we have (cf. Maeder & Meynet 2000)

$$\Gamma_\Omega(\vartheta) = \frac{F(\vartheta)}{F_{\rm lim}(\vartheta)} = \frac{\kappa(\vartheta)\,L(P)[1+\zeta(\vartheta)]}{4\pi cGM\left(1-\frac{\Omega^2}{2\pi G\rho_{\rm m}}\right)}, \quad (31)$$

where $\zeta(\vartheta)$ expresses the deviation from von Zeipel theorem due to differential rotation. This factor is in general small and here we neglect it. The mass $M_* = M(1-\frac{\Omega^2}{2\pi G\rho_{\rm m}})$ is the reduced mass, which takes into account the reduction of the gravitational potential by rotation. The ratio $\frac{\dot{I}_{\rm anis}(\overline{\Omega})}{\dot{I}_{\rm iso}(\overline{\Omega})}$ in Eq. (20) becomes

$$\frac{\dot{I}_{\rm anis}(\overline{\Omega})}{\dot{I}_{\rm iso}(\overline{\Omega})} = \frac{\int_0^\pi \frac{x^4(\vartheta)}{\cos\epsilon}\left(\frac{\Delta\dot{M}(\overline{\Omega},\vartheta)}{\Delta\sigma}\right)_{\rm anis}\sin^3\vartheta{\rm d}\vartheta}{\left(\frac{\Delta\dot{M}(\overline{\Omega})}{\Delta\sigma}\right)_{\rm iso}\int_0^\pi \frac{x^4(\vartheta)}{\cos\epsilon}\sin^3\vartheta{\rm d}\vartheta}. \quad (32)$$

Thus, we have established the various equations necessary to calculate Eq. (20).

We need however make some further comments on the normalisation constants intervening in the expressions for the mass flux. Let us first consider the isotropic case. With the above notations, the total mass loss rate can be written

$$\dot{M}_{\rm iso}(\overline{\Omega}) = \left(\frac{\Delta\dot{M}(\overline{\Omega})}{\Delta\sigma}\right)_{\rm iso} 2\pi\int_0^\pi \frac{r^2(\overline{\Omega},\vartheta)}{\cos\epsilon}\sin\vartheta{\rm d}\vartheta. \quad (33)$$

For $\dot{M}_{\rm iso}(0)$ at zero rotation, we take an expression of the mass loss rates derived observationally (cf. Kudritzki & Puls 2000; Vinck et al. 2000, 2001). To account for the fact that the observed relation is also based on rotating stars, we multiply the empirical values by a factor 0.8 (cf. Maeder & Meynet 2000) to get the average mass loss rates at zero rotation. Now, we need to obtain the global mass loss rate $\dot{M}_{\rm iso}(\overline{\Omega})$ for the rotation velocity considered. For that we use Eq. (4.29) by Maeder & Meynet (2000), which expresses the average global increase of the mass loss rates due to rotation

$$\frac{\dot{M}(\overline{\Omega})}{\dot{M}(0)} = \frac{(1-\Gamma)^{\frac{1}{\alpha}-1}}{\left[1-\frac{\Omega^2}{2\pi G\rho_{\rm m}}-\Gamma\right]^{\frac{1}{\alpha}-1}}. \quad (34)$$

If $\Omega = 0$, this ratio is of course equal to 1. The ratio $\frac{\Omega^2}{2\pi G\rho_{\rm m}} \simeq \frac{4}{9}\frac{v^2}{v_{\rm crit}^2}$ with a very good approximation. Here $v_{\rm crit}$ is the usual expression of the critical velocity. Since now $\dot{M}_{\rm iso}(\overline{\Omega})$ is known quantitatively, we may easily get from Eq. (33) the local mass flux $\left(\frac{\Delta\dot{M}(\overline{\Omega})}{\Delta\sigma}\right)_{\rm iso}$, necessary to calculate Eq. (32).

There is one more normalisation to do. For the anisotropic mass loss rate, we have

$$\dot{M}_{\rm anis}(\overline{\Omega}) = 2\pi \int_0^\pi \left(\frac{\Delta \dot{M}(\overline{\Omega},\vartheta)}{\Delta\sigma}\right)_{\rm anis} \frac{r^2(\overline{\Omega},\vartheta)}{\cos\epsilon} \sin\vartheta {\rm d}\vartheta. \quad (35)$$

Indeed, for the anisotropic mass flux we can write in a compact form $\left(\frac{\Delta \dot{M}(\overline{\Omega},\vartheta)}{\Delta\sigma}\right)_{\rm anis} = Bf(\overline{\Omega},\vartheta)$, where we put in the term B all the coefficients which do not depend explicitely on ϑ. Thus, we have

$$\dot{M}_{\rm anis}(\overline{\Omega}) = 2\pi B \int_0^\pi \frac{f(\overline{\Omega},\vartheta) r^2 \sin\vartheta}{\cos\epsilon}\, {\rm d}\vartheta. \quad (36)$$

Now, we impose

$$\dot{M}_{\rm anis}(\overline{\Omega}) = \dot{M}_{\rm iso}(\overline{\Omega}) \quad (37)$$

and in this way we can fix the value of B in Eq. (36) in a manner which is consistent with our definition of $\dot{\mathcal{L}}_{\rm excess}$ in Eq. (2). In the numerical calculations we have checked that with these prescriptions the star is losing exactly the same amount of mass in the corresponding isotropic and anisotropic cases.

Now, with these various equations, we can express $\dot{\mathcal{L}}_{\rm excess}$ in Eq. (20), which is necessary for the time dependent outer boundary condition (Eq. (19)).

5. Tests of the method and first evolutionary consequences

Here, we make some first numerical tests for the MS evolution of a fastly rotating 40 $M_\odot$ star, with an initial rotation velocity $\upsilon_{\rm ini}$ = 500 km s^{-1}. This value of the initial rotation leads to an average rotation during the MS phase of 440 km s^{-1} in the anisotropic case and to 320 km s^{-1} in the isotropic case. For this stellar mass, the opacity during the MS phase is produced by electron scattering. This means that we consider a rotating star where the anisotropy of the mass the flux given by Eq. (30) behaves like $g_{\rm eff}$. As a consequence, the higher effective gravity and $T_{\rm eff}$ at the pole imply an enhanced polar mass ejection. Other models of lower $T_{\rm eff}$ with an equatorial ring ejection, like expected for Be stars, and the various instabilities it may create (like an equatorial convective torus due to Solberg– Hoiland criterion) will be investigated in a further study.

5.1. Remarks on the accuracy

Care has to be given that the radius given by the integration of the equation of stellar structure for rotating stars as given by Meynet & Maeder (1997) is not the polar radius appearing in Eq. (26), but a radius $r_* = (\frac{3}{4\pi}V)^{\frac{1}{3}}$ where V is the volume of the distorded star. For most velocities, this radius r_* is equal to the radius $r_{(P_2)}$ at an average latitude given by $P_2(\cos\vartheta) = 0$, where P_2 is the second Legendre polynomial. At $\omega = 0.80$, r_* is larger by 0.7% than $r_{(P_2)}$, at $\omega = 0.90$, the difference reaches 1.7%.

In usual models, a very accurate description of the Ω– and μ–gradients at the edge of the convective core is necessary, because this determines the transport of chemical elements and mixing. When anisotropic winds are included as here, we need in addition to have a very accurate description of the $\Omega(r)$–profile near the stellar surface, so as to properly describe the inward transport of angular momentum by diffusion and circulation. This requires very thin shells near the stellar surface, as well as very short time steps, which enormously increases the computation time.

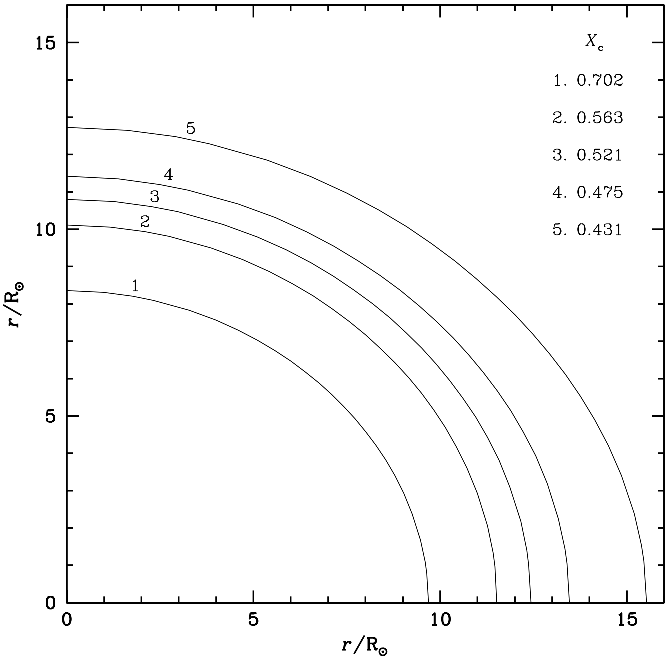

Fig. 1. Evolution of the size and shape of a 40 $M_\odot$ with an initial rotation velocity of 500 km s^{-1} during its MS phase. The average rotation during the MS phase is 440 km s^{-1}. The evolutionary stage is indicated by the value of the central hydogen content $X_{\rm c}$. We notice the stellar oblatness and its increase during evolution.

In practice, we have found that in order to obtain results which are strictly independent of the time steps Δt (which is more than desirable!), it is necessary that within one Δt, the star loses only a small fraction of the outermost shell mass,

$$\Delta t \;<\; \frac{4\pi r^2 \overline{\rho}\,\Delta r}{\dot{M}}. \quad (38)$$

Thus, high mass loss rates $\dot{M}$ imply very short time steps. We have found that typically time steps of the order of a few 10 yr. are necessary for the above model. This means that we need more than 10^5 (!) individual stellar models to cover the MS phase of massive stars.

5.2. Stellar shape and mass flux

Figure 1 illustrates the evolution of the shape of the model star during its MS phase. We notice the growth of the stellar radius and the increase of the flattening of the star as it is moving away from the zero age sequence. At the middle of the H–burning phase, the ratio of the equatorial to the polar radius is about 1.2.

The variation of $g_{\rm eff}$ over the stellar surface shown in Fig. 1 leads to the anisotropy of the mass flux (see also Pelupessy et al. 2000). The changes of the mass flux $\left(\frac{\Delta \dot{M}(\overline{\Omega},\vartheta)}{\Delta\sigma}\right)_{\rm anis}$ as a function of the colatitude ϑ are illustrated in Fig. 2 for the

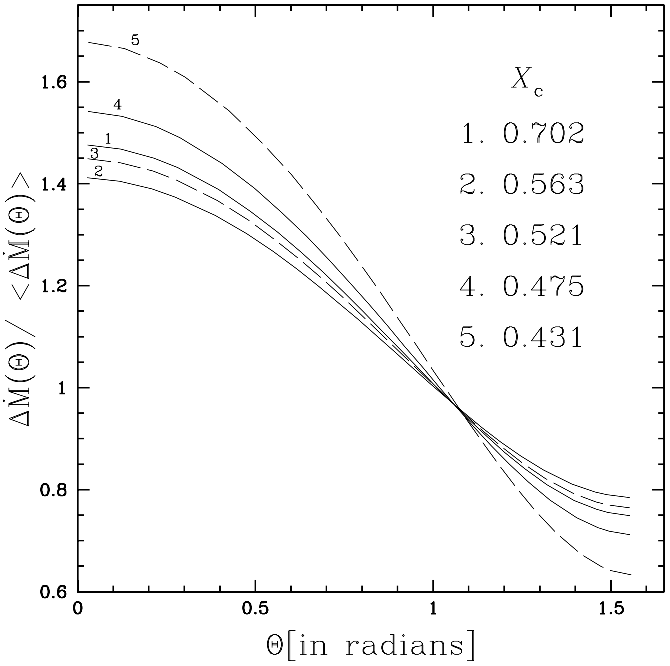

Fig. 2. Illustration of the anisotropy of the mass flux given by Eq. (30) with colatitude during the MS evolution of a 40 $M_\odot$ star with an average velocity of 440 km s^{-1}. As the masses fluxes are changing with stellar luminosity and $T_{\rm eff}$, they are normalised in each case to the average value (which is close but not identical to the value at ϑ = 1.0 radian). The horizontal axis is the colatitude ϑ in radian, i.e. the pole is to the left, the equator to the right.

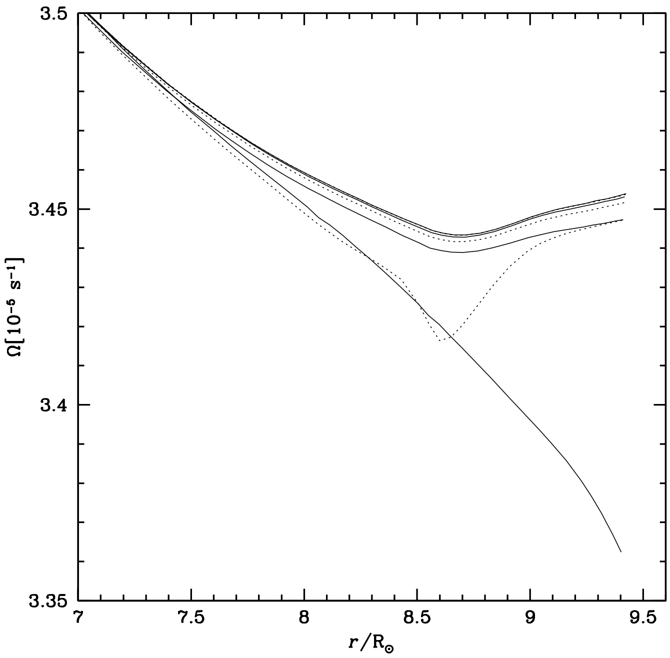

Fig. 3. Numerical tests showing the convergence of $\overline{\Omega(r)}$ near the surface towards a curve with a gradient given by Eq. (19). The sense of evolution is bottom up, with time steps of 2000 yrs. The model has 60 $M_\odot$ with an initial velocity of 300 km s^{-1}. To make the evolution of the gradient visible in this test, we apply the external torque $\dot{\mathcal{L}}_{\rm excess}$, but keep the mass constant to enable the model to reach a stationary situation.

corresponding evolutionary stages during the MS phase. We notice that despite the fact that there is no change of opacities over the stellar surface, the anisotropy is becoming rather large. In the present example, we see that the polar flux becomes equal to about 2.5 times the equatorial flux.

Such anisotropies are sufficient to produce asymmetric nebulae around hot star (cf. Lamers et al. 2001; Maeder & Desjacques 2000). For a star approaching the break–up velocity, the ratio of the polar to the equatorial $g_{\rm eff}$ may even become larger. However, at the same time the equatorial opacity would grow a lot and the resulting changes of the force multipliers, in particular of α, would also drive some strong equatorial ejection. Some models of ejected shells have been made by Maeder & Desjacques (2000).

5.3. Test of the boundary condition due to an external torque

In a stationary situation the boundary condition given by Eq. (19) determines a certain value of $\frac{\partial\overline{\Omega}}{\partial r}$ at the stellar surface corresponding to the torque $\dot{\mathcal{L}}_{\rm excess}$. This Ω– gradient can be established over a certain thickness in the very outer layers, only if the mass loss is low enough (cf. Eq. (10)), so that the concerned layers have not been ejected. Thus, such stationary situations do not apply to OB stars, but to lower mass stars and in particular to solar mass stars in case of magnetic braking.

In a star with no or little mass loss, the application of the full Eq. (6) should lead to the same result for the behaviour of Ω(r) near the surface as the boundary condition (19). As a test, we have made some numerical calculations with small time steps and a high number of shells near the surface of a 60 $M_\odot$ model at the beginning of the MS phase with an initial v = 300 km s^{-1}. We account for the complete Eq. (6) at the surface and apply the torque $\dot{\mathcal{L}}_{\rm excess}$ corresponding to the anisotropic mass loss which would normally exist. However, in order to test the boundary condition (19) we arbitrarily keep the total stellar mass constant.

Figure 3 shows some successive distributions of $\overline{\Omega}(r)$ near the stellar surface with time intervals of 2000 years. We notice the convergence of $\overline{\Omega}(r)$ toward a limiting curve in a few thousand years. As expressed by Eq. (19), for a polar enhanced mass loss we have $\frac{\partial\overline{\Omega}}{\partial r} > 0$ and this is what we observe in Fig. 3. In addition, we verify that the value of the slope $\frac{\partial\overline{\Omega}}{\partial r}$ corresponds to that given by the stationary boundary condition (19). The time necessary for establishing a stationary situation is in this case of the order of about 6000 yr, i.e. much longer that the time step Δt = a few 10 yr. during which one layer is going away. This shows that the boundary condition given by Eq. (19) may offer a consistent solution, only if the mass loss is very small. In particular, in lower mass stars there is largely enough time for a stationary gradient to be established by diffusion and circulation currents, because the considered layers are almost staying indefinitely in the star.

For O and early B–type stars, it is necessary to apply the full Eq. (6) for the boundary condition on the transport of angular momentum, with very thin shells and small time steps as mentioned above. A positive Ω– gradient may appear over a number outer layers as a result of a positive external torque. Of course, the full Eq. (6) must be applied to the extreme non stationary situations, like those of the LBV stars, where the Ω and Γ limits can be reached (cf. Maeder & Meynet 2000), or to the case of Be–stars where an equatorial shell ejection may occur.

Finally, we note that when a positive gradient $\frac{\partial \overline{\Omega}}{\partial r}$ like that in Fig. 3 can be established, it also influences the meridional circulation in the outer layers. $U(r)$ is zero at the surface, but it can become positive over a small interval below the surface, before becoming negative in somehow deeper layers due to the Gratton–Öpik term (cf. Meynet & Maeder 2000) and positive again in the deepest radiative layers surrounding the convective core. In this case, there could be 3 cells of meridional circulation between the core and the surface. The two cells with $U(r) > 0$ are rising along the rotational axis, while the intermediate cell with the negative $U(r)$ is descending along the polar axis. Thus, the account for an external torque may modify the pattern of circulation currents.

The positive Ω–gradient which arises from polar mass loss enhances the stability with respect to the Solberg–Hoiland criterion for convective–like instabilities in rotating stars. Thus, the positive $\frac{\partial \Omega}{\partial r}$ resulting from polar mass loss in OB stars brings no peculiar structural problems. This would not be true for equatorial mass loss. In this case, the negative Ω–gradient created by the equatorial mass loss may, according to the Solberg–Hoiland criterion, lead to convective instabilities in the outer equatorial layers. Such problems will be considered in a future work in relation with the case of Be–stars.

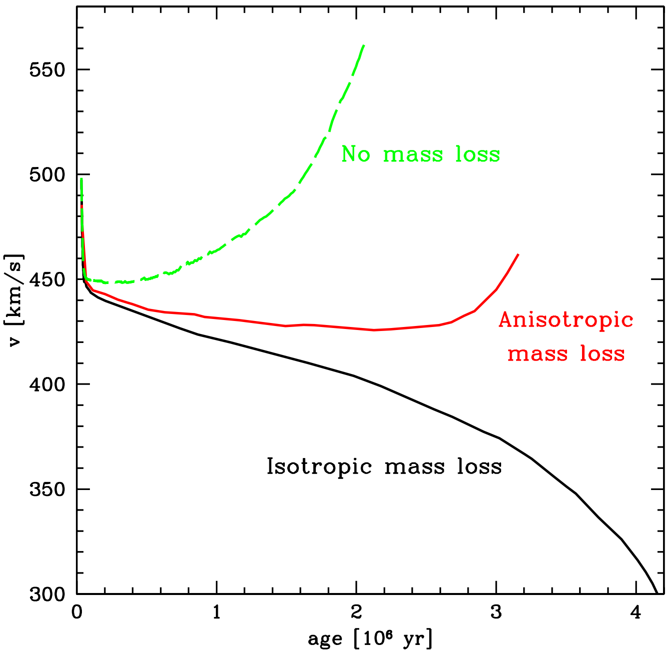

Fig. 4. Evolution as a function of time of the rotational velocity during the MS phase of a 40 $M_{\odot}$ star model starting with an initial rotation of 500 km s^{-1}. Three cases are represented, from top to bottom: the case of a rotating star without mass loss, the case of anisotropic (polar) mass loss and the case of isotropic mass loss. The two cases of no mass loss and anisotropic mass loss reach break–up and are here stopped slightly before this stage.

5.4. First evolutionary consequences

We examine some evolutionary consequences of the anisotropic mass loss with the above model of a 40 $M_{\odot}$ with the standard Pop. I composition $Z = 0.02$ and $X = 0.705$ with $\upsilon_{\rm ini} = 500$ km s^{-1}. The mass loss rates for zero rotation are those by Vink et al. (2000), which are much smaller than those by Lamers & Cassinelli (1996) used in Paper V (Meynet & Maeder 2000). Equation (34) is applied to get the global mass loss rate corresponding to the actual rotation at each time during evolution.

Due to the polar enhanced mass loss in O–stars, there is less angular momentum lost for the anisotropic than for the isotropic mass loss. As a consequence, the internal distribution of $\Omega(r)$ is slightly flatter for models with anisotropic winds than for models with isotropic winds. The reason is simple: since there is less angular momentum removed in the anisotropic winds of OB stars, the difference of Ω between the surface and the center is slightly smaller. However, these effects are small and the mixing of the chemical elements is the same in the two types of models.

Figure 4 shows the time evolution of the equatorial rotational velocity υ at the stellar surface for the isotropic and anisotropic cases during the MS phase. The case of a rotating star with the same initial velocity of 500 km s^{-1}, but without mass loss, is also shown, (this is not a model with solid body rotation; shear diffusion and meridional circulation are accounted for in this model). We notice the large differences in the evolution of υ between these 3 cases. The standard case of isotropic mass loss leads to a fastly decreasing velocity, because the isotropic mass loss is taking a lot of angular momentum away as shown by Meynet & Maeder (2000). The growth of the mass loss rates as the star is evolving makes the decrease of υ faster as the evolution proceeds. At the opposite, a model of massive star without mass loss rapidly reaches the break–up velocity. The reason is that the stellar concentration increases and the total momentum of inertia is decreasing. As a matter of fact, this last case leads to results which are not very different from those of a solid body rotating model (cf. Langer 1997), because in massive stars with a high rotation the internal coupling by circulation is very efficient. As we may have expected, the case of anisotropic mass loss is intermediate bewtween the case of no mass loss and that of isotropic mass loss. The difference between the isotropic and anisotropic cases is growing with time.

Figure 5 shows the time evolution of the ratio $\frac{\Omega}{\Omega_c}$ of the angular velocity to the critical angular velocity for the same 3 cases shown in Fig. 4. We see that, after an age of 4×10^6 yr, this ratio is fastly decreasing for the isotropic mass loss, because due to the lower $T_{\rm eff}$ of the model the mass loss rates are rapidly increasing. At the end of the MS phase, at an age of 5.8×10^6 yr the rotation velocity is only about 100 km s^{-1}. The case of the rotating model without mase loss is reaching the break–up velocity. Interestingly enough the model with anisotropic mass loss is also reaching the break–up velocity

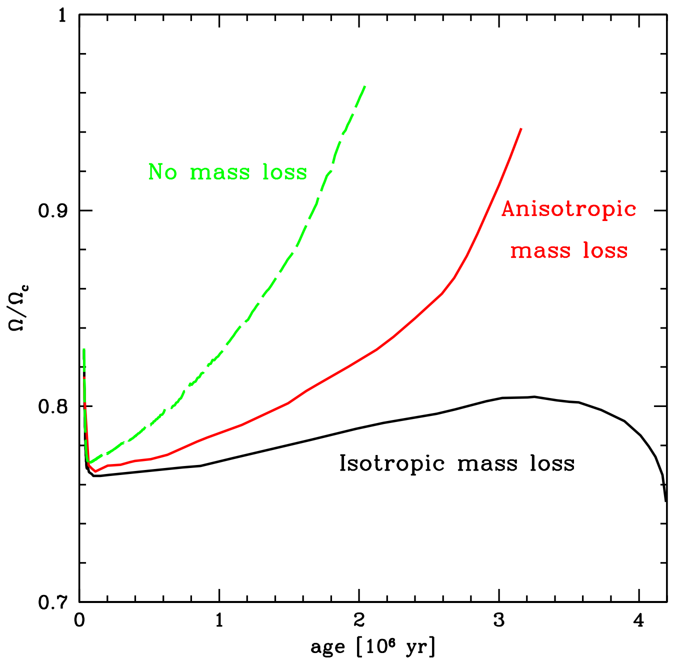

Fig. 5. Evolution of the ratio $\frac{\Omega}{\Omega_c}$ during the MS phase of a 40 $M_\odot$ star model with an initial rotation of 500 km s^{-1}. The three cases of Fig. 4 are represented.

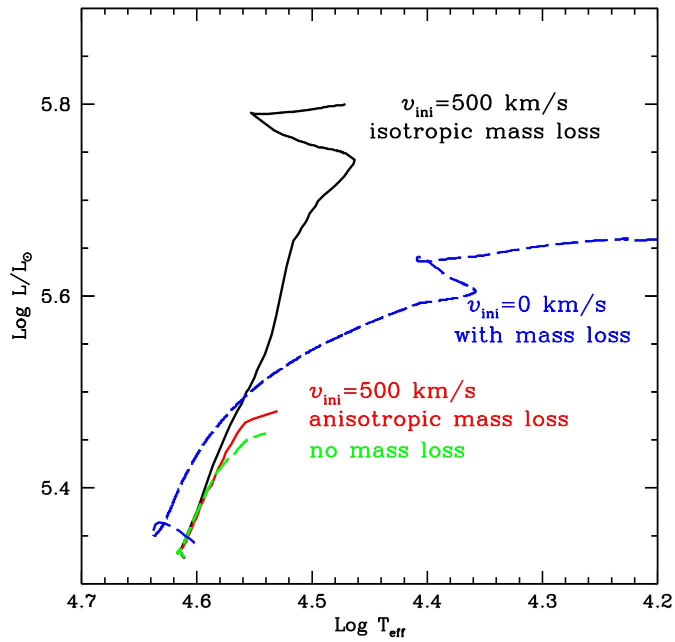

Fig. 6. HR diagram for various cases of MS evolution of a 40 $M_\odot$ at $Z = 0.02$. The 3 cases of zero, anisotropic and isotropic mass loss with an initial rotation velocity $v_{ini} = 500$ km s^{-1} are considered. In addition, a case with zero rotation (and isotropic mass loss) is shown. The two models with $v_{ini} = 500$ km s^{-1} and anisotropic mass loss or no mass loss are followed only until they reach the critical velocity. When the luminosity is $\log L/L_\odot = 5.46$, the central hydrogen content is for the models from the left to the right $X_c = 0.421, 0.467, 0.458, 0.505$.

at an age a bit larger than in the previous case. Thus, the account for anisotropies makes here a big difference with respect to the case of isotropic mass loss: instabilities may be generated, heavy mass loss will result, an equatorial shell will be ejected and the further evolution may be rather different.

The influence of the anisotropic mass loss is in general higher for faster rotation, also its importance is varying with stellar mass. For lower stellar masses, the mass loss rates are smaller and thus all the effects related to mass loss are smaller, including the effect of anisotropies. For very high masses with very high mass loss rates, it happens as discussed in Sect. 2 that the most external layers are removed before they have the time to convey the extra–torque toward the stellar interior. Tests show that the internal effects of anisotropies are negligible at 120 $M_\odot$, as well as in LBV and WR stars which have very high mass loss rates. At 60 $M_\odot$ and for an average MS velocity of 300 km s^{-1}, the difference of velocity at the middle of the MS for the two cases of isotropic and anisotropic mass loss amounts to about 20 km s^{-1}. Basically, these first tests indicate that the effects of mass loss anisotropies are significant between 25 and 60 $M_\odot$ when the average velocity on the MS is larger than 300 km s^{-1}. Further grids of models will include the effects of anisotropies and explore their size over the HR diagram.

If a star during its evolution reaches a rotational velocity close to the break–up velocity, this will enhance the mass loss according to Eq. (34). Thus at lower metallicity Z, the stars have initially less mass loss due to weaker stellar winds, and thus they may reach the break–up velocity. Paradoxically this will produce enhancements of the mass loss rates, which may become very large for stars close to the Eddington limit.

Let us also remark that for massive stars with large enough Γ, i.e. $\Gamma > 0.639$, the break-up velocity is even reached for $\frac{\Omega}{\Omega_c} < 1$, a situation which was called the Ω– or the ΩΓ–limit (cf. Langer 1997; Maeder & Meynet 2000). At the ΩΓ– limits, the star may undergo extremely high mass loss rates, which may appear as outbursts. Detailed modelisations of such events may be interesting. Let us finally mention that at the ΩΓ– limit, the expressions (30) and (34) well describes the growth of the mass flux and of the overall mass loss, because in this case the process is a radiative one. On the contrary, at the strictly speaking Ω–limit (i.e. when Γ is smaller than 0.639 and that the instability is reached only due to the fact that $\omega = 1.0$), the mass loss is not due to the radiation field and there is no detailed prediction for the mass loss rate in this case, although it is likely that the star keeps at the verge of the break–up limit (cf. Langer 1997).

Figure 6 shows the HR diagram for the 40 $M_\odot$ model with $v = 0$ km s^{-1} and mass loss, and with $v_{ini} = 500$ km s^{-1} for the 3 cases of isotropic, anisotropic and zero mass loss. We recall that in general there is an increase of the lifetimes produced by fast rotation, since the reservoir of available hydrogen is increased by rotation. In the present case, the MS lifetime until $X_c = 0$ is 4.5605×10^6 yr. for the model with $v_{ini} = 0$ km s^{-1} and it is 5.7806×10^6 yr. for the model with $v_{ini} = 500$ km s^{-1} and isotropic mass loss, i.e. 27% larger. The various tracks show significant differences. In the case with $v = 0$ km s^{-1}, the track is similar to those shown by Meynet & Maeder (2000). For $v_{ini} = 500$ km s^{-1} and isotropy, the track is going upwards to higher luminosity due to the strong mixing and the associated growth of the core. This model is keeping at a higher $T_{\rm eff}$, because mixing is bringing to the surface a lot of helium which lowers the opacity. The two models which reach critical velocity are shifted to the red due to the large atmospheric extension due to high rotation. These two models are followed here only until they reach their critical velocity, because the evolution and tracks for the star models reaching break–up very much depends on the way the losses of mass and angular momentum are treated in the critical phase. This will be further studied in forthcoming papers. For now, we just note that when the luminosity is $\log L/L_{\odot} = 5.46$, the central hydrogen content is larger for the models shifted to the right, i.e. from the model with zero rotation to the models with the highest rotation and therefore highest internal mixing. The stronger mixing keeps the central hydrogen higher.

6. Conclusion

The anisotropic mass loss by stellar winds is a complex 2–D problem, which influences stellar evolution. Here, we have devised a relatively simple method to treat carefully this problem within the context of the current 1–D stellar models.

We conclude that the anisotropic mass loss may play a significant role in the evolution of the fastest rotating OB stars. The polar enhanced mass loss rates make their rotation velocity faster during MS evolution and this may lead some stars close to the break–up limit.

For the stars with very high mass loss rates above $10^{-5}\ M_{\odot}\ {\rm yr}^{-1}$, as is the case for OB stars with masses higher than 60 $M_{\odot}$, for WR stars and LBV stars, the anisotropic mass loss will shape and determine the evolution of the surrounding nebulae (Lamers et al. 2001), but will have little effect on the internal evolution, because the extra–torques due to the anisotropies have not the time to be transmitted inward by shear turbulence and circulation before the concerned layers are ejected.

For rotating stars with $T_{\rm eff}$ lower than about 21 000 K, an equatorial ejection may occur and have important consequences for the further evolution of the stellar angular momentum and for the instabilities oin the outer layers.

Acknowledgements. I express my gratitude to Dr. Georges Meynet for his many encouragements and for his great help during this work.

References

Castor, J. I., Abbott, D. C., & Klein, R. I. 1975, ApJ, 195, 157
Kudritzki, R. P., & Puls, J. 2000, ARA&A, 38, 613
Lamers, H., & Cassinelli, J. P. 1996, in Mass Loss from Stars, ed. C. Leitherer, U. Fritze-von-Alvensleben, & J. Huchra, From Stars to Galaxies: The Impact of Stellar Physics on Galaxy Evolution, ASP Conf. Ser., 98, 162
Lamers, H. G. L. M., Snow, T. P., & Lindholm, D. M. 1995, ApJ, 455, 269
Lamers, H. J. G. L. M., Nota, A., Panagia, N., Smith, L., & Langer, N. 2001, A&A, 369, 574
Langer, N. 1997, in Luminous Blue Variables: massive stars in transition, ed. A. Nota, & H. J. G. L. M. Lamers, ASP Conf. Ser., 120, 83
Maeder, A. 1999, A&A, 347, 185 (Paper IV)
Maeder, A. 2002, A&A, in press
Maeder, A., & Meynet, G. 2000, A&A, 361, 159 (Paper VI)
Maeder, A., & Meynet, G. 2001, A&A, 373, 555 (Paper VII)
Maeder, A., & Desjacques, V. 2000, A&A, 372, L9
Maeder, A., & Zahn, J. P. 1998, A&A, 334, 1000 (Paper III)
Meynet, G., & Maeder, A. 1997, A&A, 321, 465 (Paper I)
Meynet, G., & Maeder, A. 2000, A&A, 361, 101 (Paper V)
Nota, A., & Clampin, M. 1997, in Luminous Blue Variables: massive stars in transition, ed. A. Nota, & H. J. G. L. M. Lamers, ASP Conf. Ser., 120, 303
Pelupessy, T., Lamers, H. J. G. L. M., & Vink, J. S. 2000, A&A, 359, 695
Petrenz, P., & Puls, J. 2000, A&A, 358, 956
Puls, J., Kudritzki, R. P., Herrero, A., et al. 1996, A&A, 305, 171
Talon, S., Zahn, J. P., Maeder, A., & Meynet, G. 1997, A&A, 322, 209
Vink, J. S., de Koter, A., & Lamers, H. J. G. L. M. 2000, A&A, 362, 295
Vink, J. S., de Koter, A., & Lamers, H. J. G. L. M. 2001, A&A, 369, 574
von Zeipel, H. 1924, MNRAS, 84, 665
Zahn, J. P. 1992, A&A, 265, 115